

Contents list available at CBIORE journal website

# Remarkable Energy Development

Journal homepage: https://ijred.cbiore.id



**Research Article** 

# N/S-doped carbon electrode derived from paper waste as a sustainable electric double-layer capacitor

Fitria Rahmawati<sup>a,b</sup>, Nur Aini<sup>a</sup>, Qanita Ridwan<sup>a</sup>, I Gusti Ayu Filia Paramartha<sup>a</sup>, Denis Octareta Amelia Putri<sup>a</sup>, Dini Deviana Saputri<sup>a</sup>, Khoirina Dwi Nugrahaningtyas<sup>a,b</sup>, Eddy Heraldy<sup>a,b</sup>, Yuniawan Hidayat<sup>a,b</sup>, I.F. Nurcahyo<sup>a,b</sup>, Ivandini Tribidasari Anggraningrum<sup>c</sup>

**Abstract**. This research aims to produce N/S-doped Carbon Electrode derived from paper waste (NSCEp) for Electric Double-Layer Capacitor (EDLC). The paper waste holds potential as raw material for carbon production because of its high cellulose content, abundance of availability, and low price. To enhance the electrical performance of the carbon, an activation step was conducted, followed by double doping with nitrogen and sulfur using thiourea. The NSCEp result was analysed to examine its specific diffraction peaks, crystallinity, morphology, and elemental contents. The NSCEp powder was then mixed with dispersant to produce a homogeneous slurry for the electrode film. The EDLC was assembled in a sandwich-like structure, with sodium hydroxide (NaOH) solution impregnated in a separator between the carbon film electrodes. The EDLC assembly was conducted under an argon atmosphere in a CR2032 coin cell. The results found that the NSCEp provides a high electrical conductivity of 1.21 x 102 S/cm. The prepared EDLC achieved the specific capacitance value of 39.555 F/g as determined by cyclic voltammetry (CV) analysis. Furthermore, the EDLC demonstrates high initial charge-discharge capacities of 300.56 mAh/g and 248.88 mAh/g, respectively, at a current of 0.015 A/g. The capacity remains stable for up to 300 charge-discharge cycles.

Keywords: Paper Waste, Activated Carbon, Electrode, Capacitor, Biomass



@ The author(s). Published by CBIORE. This is an open access article under the CC BY-SA license (http://creativecommons.org/licenses/by-sa/4.0/).

Received: 16th Nov 2024; Revised: 5th January 2025; Accepted: 26th February 2025; Available online: 5th February 2025

# 1. Introduction

The excessive global use of paper contributes to environmental unsustainability, leading to ecological disruptions, climate change due to deforestation, and the release of harmful toxic substances (Karakilic et al., 2023; Singh, Kumar, & Chandra, 2022; Yousufi, 2023). The consumption of paper, along with the pulp and paper production process, has become the fourth largest energy consumer worldwide, causing a significant environmental impact (Man et al., 2023). According to the Food Agriculture Organization (FAO) (2023). manufacturing of wood-based boards is estimated to be around 396.3 million cubic meters per year (Konukcu & Engin, 2024). In the meantime, the Ministry of Environment and Forestry of Indonesia indicated that paper waste comprised 12% of the total 67.8 million tons of waste produced in 2020 (Saputra, Rhohman, & Fauzi, 2022). Responding to this matter, the global community is committed to reducing the use of paper-based documents, although certain sectors like education, offices, and industries continue to rely on paper (Prasetyo, Damaraji, & Kusumawardani, 2020). For instance, the packaging industry (Keskin, Altay, Kurt, & Fleming, 2020), households (Łatka et al., 2022), and hotels produce a significant of tissue paper waste

(Hanafiah *et al.*, 2019). It is predicted that global consumption of pulp and paper will double between 2010 and 2060, along with the volume of paper waste. This is because most paper products eventually end up in landfills, resulting in a staggering amount of paper waste.

Paper offers the benefits of being bio-based, biodegradable, and recyclable (Oloyede & Lignou, 2021). It is well established that paper consists of cellulose (60-70%), hemicellulose (10-20%), and lignin (~5%) (V. Kumar, Pathak, & Bhardwaj, 2020). Cellulose is a fundamental component of lignocellulosic materials, which are commonly used as precursors for carbonbased materials, especially for activated carbon (Ahmad & Azam, 2019; Suhas et al., 2016). Carbon-based materials are widely accessible and hold great promise across numerous fields due to their outstanding spectroscopic, mechanical, thermal, and electrochemical characteristics (Soleymani et al., 2021). Using a "green" carbon precursor presents an alternative method for synthesizing carbon material which offers a costeffective, durable, energy-efficient, and reducing pathogen presence (Saputri, Jan'ah, & Saraswati, 2020). Activated carbon (AC) is a carbonized material renowned for its large specific surface area, high porosity, favourable surface functionalization, good chemical stability, high electrical conductivity, and less

\* Corresponding author(s)

Email: fitria@mipa.uns.ac.id (F. Rahmawati)

<sup>&</sup>lt;sup>a</sup>Department of Chemistry, Faculty of Mathematics and Natural Sciences, Sebelas Maret University, Jl. Ir. Sutami 36A Kentingan, 57126, Surakarta, Indonesia <sup>b</sup>Research Group of Solid State Chemistry & Catalysis, Chemistry Department, Sebelas Maret University, Jl. Ir. Sutami 36A Kentingan, 57126, Surakarta, Indonesia

<sup>&</sup>lt;sup>c</sup>Department of Chemistry, Faculty of Mathematics and Natural Sciences, Universitas Indonesia, Depok, 16425, Indonesia

expensive (Y. Gao, Yue, Gao, & Li, 2020; Nille et al., 2021; Tumimomor, Maddu, & Pari, 2017). AC becomes the raw material for electrodes in various devices, including ion detectors (Guan et al., 2020; Heliani, Rahmawati, & Wijayanta, 2024), adsorbents (Ahmed, Hameed, & Khan, 2023; Kamboj & Tiwari, 2024), secondary batteries (Yun Chen, Guo, Liu, Zhu, & Ma, 2021; Tonoya et al., 2023), and capacitors or supercapacitors (Lobato-Peralta et al., 2023; Manimekala, Sivasubramanian, Karthikeyan, & Dharmalingam, 2023). Various types of biomasses can be converted into sustainable AC, including pine nuts (Mestre, Viegas, Mesquita, Rosa, & Carvalho, 2022; Sen et al., 2024), bamboo (Cheng et al., 2023; Duan et al., 2023), lotus calyx (Dhakal et al., 2022), tea waste (Hossain, Islam, Rahaman, Khatun, & Matin, 2023; Mariah, Rovina, Vonnie, & Erna, 2023), sugarcane solid waste (Rahmawati et al., 2023), coffee waste (Aouay, Attia, Dammak, Ben Amar, & Deratani, 2024; Chiang, Chen, & Lin, 2020), tobacco waste (Chipembere, Biswick, & Vunain, 2024; Gonçalves Jr et al., 2023), and wood waste (Alahabadi et al., 2020; Boulanger, Talyzin, Xiong, Hultberg, & Grimm, 2024).

A supercapacitor is a device used for energy storage focused on achieving high capacity, high power density, good cycle life, fast charge-discharge performance, and controlled energy density (Olabi, Abbas, Al Makky, & Abdelkareem, 2022; Pameté et al., 2023; Rajpurohit, Punde, Rawool, & Srivastava, 2019; Rudra, Seo, Sarker, & Kim, 2024). The performance of a supercapacitor is influenced by factors, such as the selection of electrodes and the fabrication methods used (Khan, Ryu, & In, 2024). Supercapacitors are divided into three types: electric double-layer capacitors, pseudo-capacitors, and hybrid capacitors, depending on the charging mechanism (Sharma & Chand, 2023). Electric Double-Layer Capacitors (EDLCs) become promising future electrical energy storage devices due to their use of porous carbon materials, which enhance energy density, extend lifespan, improve performance, and reduce production costs compared to pseudo-capacitors (Jia et al., 2019; I. Yang et al., 2020). The physical process of adsorption and desorption of cations and anions occurs reversibly at the electrode-electrolyte interface, resulting in charge storage in EDLCs. This is also related to an electrostatic process. It does not happen through the chemical charge transfer reaction or phase changes during the charging and discharging. The available surface area of the electrode material plays an important role in the capacitance of EDLC. Thus, carbon materials (carbon nanotubes, nanosheets, and biomass-derived heteroatom-doped carbons) are needed because of their excellent potential electrical conductivity, large surface area, and chemical stability (Lim et al., 2023; Samage, Halakarni, Yoon, & Sanna Kotrappanavar, 2024; Q. Wu et al., 2021; Zhai et al., 2022).

Improving the energy density without compromising power density, is a challenge for supercapacitor research (Revathi, Palanisamy, Boopathiraja, & Sudha, 2024). To enhance electrochemical performance, increasing energy density remains a critical focus, while maintaining high electrical conductivity is essential. This can be achieved by integrating porous carbon materials with metal oxides (such as MnO<sub>2</sub>, Fe<sub>2</sub>O<sub>3</sub>, NiO, Co<sub>3</sub>O<sub>4</sub>, RuO<sub>2</sub>, and NiCo<sub>2</sub>O<sub>4</sub>), incorporating heteroatom doping (with elements like N, P, S, and O), and adding conductive polymers (Arumugam, Mayakrishnan, Subburayan Manickavasagam, Kim, & Vanaraj, 2023; K. Yang *et al.*, 2023). Introducing heteroatoms through doping can modify the chemical inertness by disturbing the electron structure of sp<sup>2</sup> hybrid carbon (Ait El Fakir, Anfar, Enneiymy, Jada, & El Alem, 2022). Doping carbon materials with heteroatoms (N, P, S, and

O) is a potential approach to enhance the surface wettability of the carbon, improve electron conductivity, and increase specific capacitance, and rate capability (Gopalakrishnan & Badhulika, 2020; Liu *et al.*, 2024). Doping can be performed in two distinct method: external doping (requiring additional precursors as doping agents) and self-doping (employing a direct pyrolysis method) (Gopalakrishnan & Badhulika, 2021).

Nitrogen and sulfur are the most extensively studied dopants for carbon-based materials among the various heteroatoms. Nitrogen atoms could boost carbon material's electronic conductivity and cycling performance (S. Wu et al., 2021). The conjugation between the  $\pi$ -system of the carbon lattice and nitrogen lone pairs can greatly influence the physicochemical properties of activated carbon. Graphitic nitrogen enhances electron transfer in the carbon lattice, while pyridinic and pyrrolic nitrogen improve faradaic reaction sites due to nitrogen's higher electronegativity (M. Chen, Le, Zhou, Kang, & Yang, 2020; Uppugalla, Pothu, Boddula, Desai, & Al-Qahtani, 2023). Sulfur, despite having similar electronegativity to carbon, could improve electronic properties, polarize electron pairs, create charge sites, and enhance surface affinity to electrolytes and electrochemical performance due to its larger size (M. Chen et al., 2020). Sulfur shows greater electrochemical activity than nitrogen by disrupting the carbon framework's electron density (Domínguez-Ramos et al., 2022; S. Wu et al., 2021). Instead of using a singular atom, the combination of two heteroatoms (dual doping of N and S) will give a synergistic effect to improve the electrochemical performance by expanding the pore size and the defects (F. Gao et al., 2024; Wang, Huang, Sun, Yang, & Sillanpää, 2021). Thiourea as a cheap and safe chemical becomes a potential candidate with very high nitrogen (36.8 wt%) and sulfur contents (42.1 wt%) which can be used for nitrogen and sulfur doping in activated carbon (Cui et al., 2022). The previous research has been developed to produce N/S-doped porous carbon sheets derived from newspaper waste (Yuwei Chen et al., 2019), N/S-doped carbon electrode from a carbonized bagasse using thiourea (Rahmawati, Amalia, Ridassepri, Nakamura, & Lee, 2024), and N/S-doped activated carbon derived from palm waste with thiourea for supercapacitor (Rustamaji et al., 2024).

In this study, nitrogen and sulfur (N/S) atoms were doped into activated carbon derived from paper waste. The activation was performed using a chemical method with sodium hydroxide, followed by N/S doping through a reaction with thiourea in ethanol. The resulting material, referred to as N/S-doped Carbon Electrode from Paper (NSCEp), was used as an electrode in a CR2032 coin cell capacitor. The synthesized material was characterized to evaluate its structural, morphological, and electrochemical properties.

#### 2. Experimental Methods

# 2.1. Materials

The material utilized in this research were scrap paper waste from food box papers (procured from a second-hand goods dealer in the Jebres District, Surakarta, Central Java, Indonesia), ethanol (70%, General Labora), hydrochloric acid (HCl, Merck, 37%), sodium hydroxide (NaOH, Merck), thiourea (99.0%, Tianjin Damao Chemical Reagent Factory), N-methyl-2-pyrrolidone (NMP, KGC Saintifik, West Jakarta), Acetylene Black (KGC Saintifik, West Jakarta), polyvinylidene fluoride (PVDF, KGC Saintifik, West Jakarta), Al foil (KGC Saintifik,



Fig. 1 Setup of capacitor (EDLC) assembling in a CR2032 coin cell

West Jakarta), Cu foil (KGC Saintifik, West Jakarta), Whatman filter paper grade 42, nitrogen ( $N_2$  gas, Industrial Grade, Samator, Indonesia), argon (Ar gas, Ultra High Purity (UHP), 99.99%, Samator, Indonesia), silver paste (SPI Supplies), and distilled water. Some tools that were used in this research were the casting machine (TMAXCN), vacuum oven (DZF-6010), and Argon glove box (KF-40 VGB-1).

#### 2.2. Preparation of Activated Carbon (AC) from Paper Waste

Paper waste as the raw material for carbon powder preparation, was washed and soaked in distilled water for 24 hours. After being filtered from water, the residue was dried at  $110^{\circ}$ C for 24 hours to produce dried paper waste. The dried paper waste was then subsequently carbonized at  $800^{\circ}$ C for 2 hours in a nitrogen (N<sub>2</sub>) gas flow. The carbonized material was then activated using a sodium hydroxide (NaOH solution), with a ratio of 1:5 (mass to volume) for the carbonized material and the NaOH solution, respectively.

#### 2.2 Preparation of N/S-doped Carbon Electrode (NSCEp)

Nitrogen and sulfur (N/S) were doped into the activated carbon by mixing it with a thiourea (99.0%, Tianjin Damao Chemical Reagent Factory) solution in ethanol (70%, General Labora), using a mass ratio of 2:1 for the activated carbon and thiourea. The mixture was stirred for two hours and then heated in an oven at 80°C for 6 hours to produce a dried sediment. This sediment was then heated at 850°C for 2 hours under a nitrogen gas flow (N2, Industrial Grade, Samator, Indonesia), resulting the NSCEp.

The paper waste, carbonized paper, activated carbon and NSCEp were analyzed using Fourier-Transform Infrared (FTIR, Shimadzu Prestige-21, Japan) to identify the functional groups present. The X-ray diffraction analysis (XRD, Rigaku Miniflex 600, Japan) was performed to understand the diffraction patterns compared with standard phase diffraction. The Scanning Electron Microscope (SEM, JEOL JSM 6510 LA, Japan) and Transmission Electron Microscope (TEM, JEOL JEM-1400, Japan) were employed to study the surface and microstructure morphology of material. The Energy Dispersive X-ray Spectrocopy (EDX, JEOL JSM 6510 LA, Japan) assessed the elemental composition of the sample. The surface area, pore volume, and pore size distribution were analyzed by the Surface Area Analyzer (SAA, Quantachrome Instruments TouchWin V1.2, Type NOVA Touch 4LX, USA), through adsorptiondesorption of N2 gas at 77K and relative pressure by using Brunauer-Emmett-Teller (BET) and Barrett-Joyner-Halenda (BJH) methods.

# 2.2 Fabrication of Carbon Electrode Film and Capacitor Assembly

A slurry of NSCEp, acetylene black, and polyvinylidene fluoride were prepared in a 7:2:1 ratio, respectively. The mixture was

ground with an agate pestle for 30 minutes to create mixture A. N-methyl-2-pyrrolidone (NMP) dispersant was then added to mixture A at a ratio of 5 mL per 1 gram, resulting in mixture B, which was stirred at room temperature. Mixture B was continuously stirred for 2 hours to achieve a homogeneous carbon ink, which was then applied onto Cu and Al foils using a casting machine with a thickness of 45 mm. The carbon sheets were then dried in a vacuum oven at 80°C for 12 hours to create carbon electrodes, making them ready for capacitor assembly.

The capacitor assembly took place inside an argon glove box, following the setup shown in **Fig. 1**. The capacitor was assembled in a CR2032 coin cell, with a separator placed between the Carbon/Cu and Carbon/Al electrodes. The separator used was Whatman paper soaked in a 6 M NaOH solution.

#### 2.2 Electrochemical Test

Impedance analysis was performed on the prepared carbon sheet within the frequency range of 20 Hz to 100 kHz (using an EUCOL LCR meter 20 Hz – 5 MHz) to evaluate its electrical conductivity. The impedance data was fitted using *ZView software*, and the conductivity was calculated using equation (1), where  $\sigma$  represents the specific conductivity (S·cm<sup>-1</sup>), l denotes the distance between the two electrode spots (cm), and A is the area of the active electrode or the silver paste (cm<sup>2</sup>).

$$\sigma = \frac{1}{R} \frac{l}{A} \tag{1}$$

Cyclic Voltammetry (Electrochemical Workstation CS150, Wuhan Corrtest Instruments, China) analysis to the capacitor was done to understand electrode performance under potential range of -2 to 0.8 V vs Na $^+$ /Na under scan rate of 50 mV/s. Galvanostatic Charge-Discharge (NEWARE 5V1A, Neware Technology Ltd., China) analyze the reversible specific capacity (mAh/g), and cycle ability under current drawn of 0.015 A/g, 0.15 A/g, 1.5 A/g, and potential range of 0.0 – 1.0 V.

## 3. Result and Discussion

#### 3.1. Characterization of Carbonized Material

Paper waste had been successfully processed into carbonized material and activated by reacting with sodium hydroxide solution, then doped with nitrogen and sulfur to produce NSCEp as electrode material for EDLC application. Fig. 2 shows the schematic representation of NSCEp production. The carbonization process at 800°C provides the degradation structure of cellulose, hemicellulose, lignin, and other compounds as the paper component into carbon's graphitization, releasing the unreacted volatile components carried out by nitrogen flows (Rahmawati et al., 2021). The chemical activation aims to obtain porous carbon along with the main goal of achieving material with a high surface area (Yuan et al., 2020). The N/S-doped Carbon Electrode from Paper (NSCEp) chemical structure in Fig. 2 is depicted based on the previous research (Rahmawati et al., 2024). This research found that the carbonization and activation yield of activated carbon obtained up to 24.13% from the initial paper's weight. Meanwhile, the weight reduction from carbonized char to activated carbon was only 2.6% or resulting 97.4% rendement. It indicates that the weight reduction mostly occurred during carbonization because of cellulose, lignin, and some unstable compound degradation.

Fourier-transform infrared spectroscopy (FTIR) was applied to analyze the functional group that arranged the prepared paper waste, carbonized paper, activated carbon (AC), and

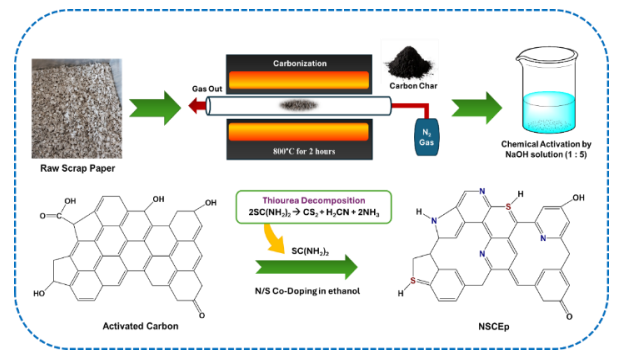
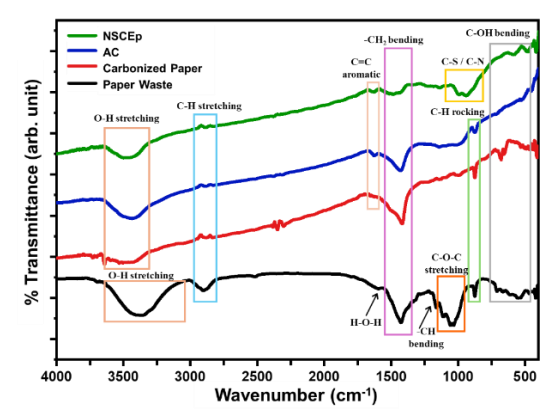


Fig. 2 Schematic representation of N/S-doped Carbon Electrode from Paper (NSCEp) production

NSCEp (Fig. 3). Paper waste exhibited some transmission peaks at 701 cm<sup>-1</sup> refers to C-OH bending, C-H rocking at 878 cm<sup>-1</sup> (Md Salim, Asik, & Sarjadi, 2021), C-O-C stretching at 1066 cm<sup>-1</sup> <sup>1</sup>, -CH<sub>2</sub> bending at 1427 cm<sup>-1</sup> (Manandhar, Shrestha, Sciortino, Ariga, & Shrestha, 2022), C-H stretching at 2898 cm<sup>-1</sup> (Hegde & Bhat, 2024), and O-H stretching at 3374 cm<sup>-1</sup> (Singla *et al.*, 2024). Those peaks represent the functional group of cellulose, hemicellulose, lignin, and some compound structures. The breaking down of the cellulose compound into carbon is confirmed by the appearance of the C=C aromatic peak at 1619 cm-1 (L. Chen et al., 2024), the shift of the O-H stretching peak to 3445 cm<sup>-1</sup>, and the lower peak intensity of C-H stretching. The peak of C=C aromatic indicated the success of carbonization due to the heating process up to 800°C. The decreasing intensity of C-H stretching and the shift in O-H stretching suggest that C-H bonds contribute to graphitization, leading to the formation of a C=C aromatic structure. This reduction in C-H peaks further indicates the loss of hydrogen atoms as the material transitions to a more graphitic framework (Qin et al., 2022). Compared to carbonized paper, activated carbon exhibits a higher peak intensity of O-H stretching, indicating the successful activation through the insertion of more O-H into the C=C structure. Furthermore, nitrogen (N) and sulfur (S) doping into the activated carbon to produce NSCEp, is revealed by the appearance of the C-S peak at 937 cm<sup>-1</sup> (J. Chen et al., 2025) and C-N peak at 998 cm<sup>-1</sup> (Luo et al., 2018). As seen from the FTIR investigation, the derived activated carbon displayed the incorporation of nitrogen and sulfur atoms, which played a role in the creation of bonds within its structural framework (Rustamaji et al., 2024).

The X-Ray Diffraction (XRD) analysis was conducted to confirm the crystal structure and chemical properties of the



**Fig. 3** FTIR analysis of paper waste, carbonized paper, activated carbon (AC), and N,S-doped Carbon Electrode from Paper (NSCEp)

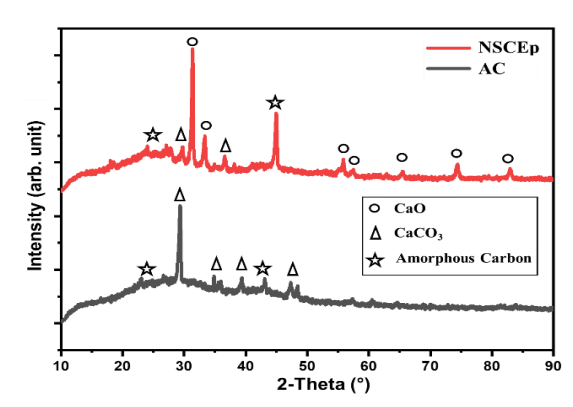


Fig. 4 XRD analysis of AC and NSCEp

activated carbon (AC) and the NSCEp produced. Paper waste is known to contain not only cellulose, hemicellulose, and lignin, but also several potential mineral compounds like calcium carbonate (CaCO<sub>3</sub>), silicon dioxide (SiO<sub>2</sub>), magnesium oxide (MgO), and aluminium oxide (Al2O3), as the following result from the elemental composition. Calcium carbonate, or calcite, is typically the dominant component due to its use as a filler in papermaking (Palanichamy, Venkatachalam, & Gupta, 2023). As shown in Fig. 4, the XRD spectra of activated carbon and NSCEp display a sharp peak that indicates a crystalline structure. The broad peaks at 20 angles of 25° and 44° are attributed to amorphous carbon phases based on JCPDS #41-1487 (Rahmawati et al., 2024), while another crystalline peak likely corresponds to the calcite (CaCO<sub>3</sub>) structure based on JCPDS #05-0586 (Ma et al., 2013). After nitrogen and sulfur doping, the calcite transforms into a calcium oxide (CaO) phase based on JCPDS #37-1497 (Scialla et al., 2020), due to the heating process.

The Raman spectra (Fig. 5) of activated carbon and NSCEp show two main peaks at ~1340 cm<sup>-1</sup> and ~1590 cm<sup>-1</sup> as a characteristic result of carbon material for the disorder (D band) and graphite (G band). The D band usually appears at 1250-1450 cm<sup>-1</sup>, indicating the presence of C-C sp<sup>3</sup> bonds. This band is related to structural defects or disorders in activated carbon due to the incorporation of active groups along the graphite carbon structure. The D band peak results from A1g symmetry vibrations, reflecting structural irregularities. On the other hand, the G band is typically observed in the Raman shift range of 1575-1590 cm<sup>-1</sup>, representing a tangential mode associated with the stretching of C=C sp2 bonds in a hexagonal graphite lattice. The G band peak is attributed to the asymmetric planar stretching vibrations of C=C bonds with E2g symmetry (Gakis, Termine, Trompeta, Aviziotis, & Charitidis, 2022; Gergeroglu & Ebeoglugil, 2022). The successful indication of doping N/S is by measuring the ratio intensity of the D and G bands. The intensity ratio of the D and G bands (ID/IG) reflects the level of carbon defects, with a higher ratio indicating a greater degree of structural defects. The N/S doping raised the I<sub>D</sub>/I<sub>G</sub> ratio from 0.884 before doping to 1.039, signifying an increase in defects after the doping process (Rahmawati et al., 2024).

The optical images in Fig. 6 (a, d, and g) show carbon, activated carbon, and NSCEp sample results. The carbonized material displays a rough powder structure, while the activated carbon and NSCEp exhibit a more refined particle powder form. The Scanning Electron Microscope (SEM) images show the morphological structure of the materials: Fig. 6 (b and c) for carbon, Fig. 6 (e and f) for activated carbon, and Fig. 6 (h and i) for NSCEp. The carbonized material obtained from waste exhibits features, such as channels, pores, cavities, and cracks on its outer surface (Çiftçi, Çalışkan, İçtüzer, & Arslanoğlu,

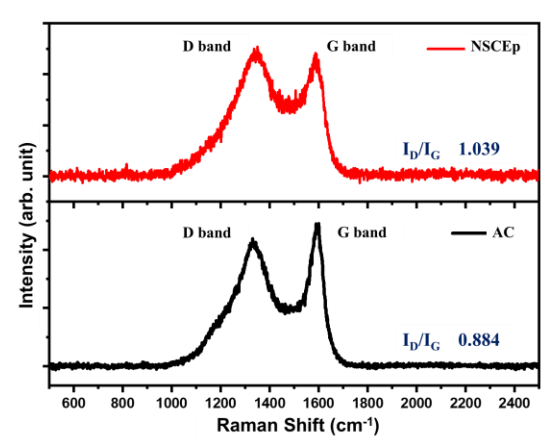
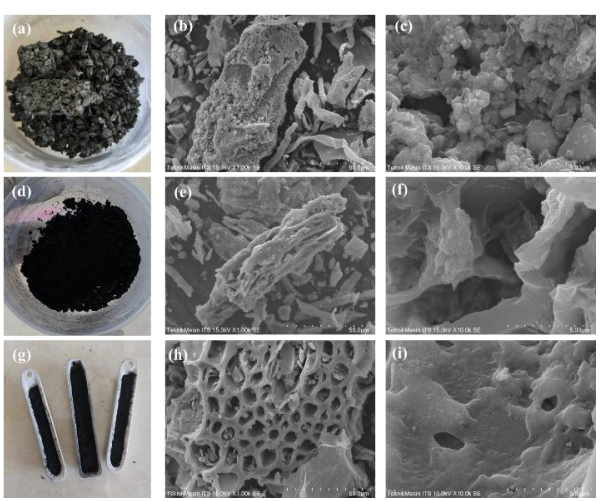


Fig. 5 Raman analysis of AC and NSCEp

2024). It can be seen from Fig. 6 (b) that the carbonized paper forms irregularly rough flakes with non-homogenous pores as seen in Fig. 6 (c) (Rahmawati et al., 2023). The activation of carbon facilitates the interaction between carbonized material and other compounds, rearranges the structure, and increases the pore's shape and distribution of carbon (Singla et al., 2024). It impacts the corroding of the carbon skeleton, which helps develop pores as functional for buffering the electrolyte, aids in ion diffusion, and enables quick ion transport to the inner surface (Hegde & Bhat, 2024). Fig. 6 (e-f) for activated carbon shows the better formation of pores, indicating the activation process's accomplishment. The activation process of carbon is accomplished by the appearance of better pores in Fig. 6 (e-f), which is expected to improve its surface area and adsorption capacity. Fig. 6 (h-i) represents the 3D honeycomb-shaped porous structure of NSCEp with 3.5 µm pore's diameter (S. Kumar et al., 2023). The microporous contributes to good electrolyte access to electrodes that will increase the capacitor performance.

The Energy-Dispersive X-ray (EDX) mapping is displayed in Fig. 7 with the atomic percent of elemental composition. The carbonized paper shows the result that mainly composed of C (26.78%), O (53.66%), Ca (13.64%), Si (1.20%), Mg (0.48%), and N (2.75%). It is correlated with the XRD result that paper waste waste consists of another potential mineral compound. The activation process increases the carbon (C) composition up to



**Fig. 6** The optical image of (a) carbonized paper, (b, c) SEM images of carbonized paper, (d) optical image of AC, (e, f) SEM images of AC, (g) optical image of NSCEp, and (h, i) SEM images of NSCEp

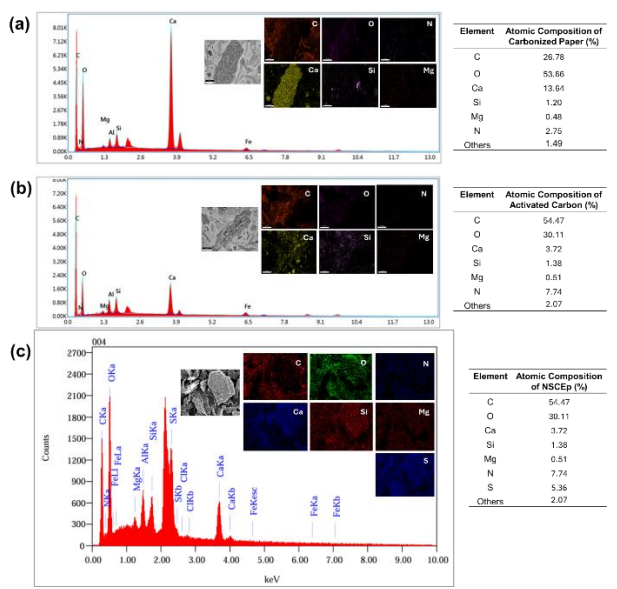


Fig. 7 EDX-mapping and elemental composition of (a) carbonized paper, (b) activated carbon (AC), and (c) NSCEp

54.47%, and decreases the mineral compound. It can be concluded that the activation process removes the impurities component and changes the interconnection of carbon with the active sites. The N/S doping to activated carbon is proven by the exhibition of sulfur (S) composition (5.36%) and nitrogen (N) composition (2.78%). The decreasing of carbon composition implies the etching of sulfur and nitrogen atoms into the hexagonal graphene structure, breaking the C=C chain with the insertion of S and N (the formation of C-S and C-N bonding as described in FTIR explanation).

The Transmission Electron Microscope (TEM) of activated carbon and NSCEp is visualized in Fig. 8 (a-f) for activated carbon and Fig. 8 (g-l) for NSCEp. Activated carbon can be formed in micro-, meso-, and macro-porous characteristics (Ghafourian, Zare, Sharif, & Zamani, 2019). The microporesmacropores structure is useful for electrons and ions exchange under high-rate discharge. The micropores are not expected to quickly transport electrolyte ions because of their high resistance. However, the mesoporous structure offers pathways for ions to access the micropores, which supports the energy storage of supercapacitors (Chai et al., 2022). Activated carbon is dominantly distributed by mesoporous structures with the pore size under 50 nm. Meanwhile, the NSCEp shows various microporous, mesoporous, and microporous structures. It shows the crystalline structure which is possibly coming from a graphene-sheet-like structure layer. The hexagonal molecular form of the NSCEp was achieved through a heating process up to 850°C during the doping step to form a graphite structure. The pores generally take the form of spherical particles.

The Surface Area Analysis (SAA) shows the material's adsorption and desorption isotherm behaviour, characterized by a hysteresis loop at a relative pressure above 0.1 P/Po, confirming the occurrence of physical adsorption. Adsorption is the process where ions, molecules, or atoms attach to a surface, while desorption refers to the removal of the previously adsorbed substance. The isotherm curve of carbon, activated carbon, and NSCEp is shown in Fig. 9 (a). Carbonized paper, activated carbon, and NSCEp samples all exhibit an S-shaped curve, classified as type IV, which is characteristic of water adsorption on hydrophobic microporous-mesoporous adsorbents (Ridassepri et al., 2020). A steeper adsorption

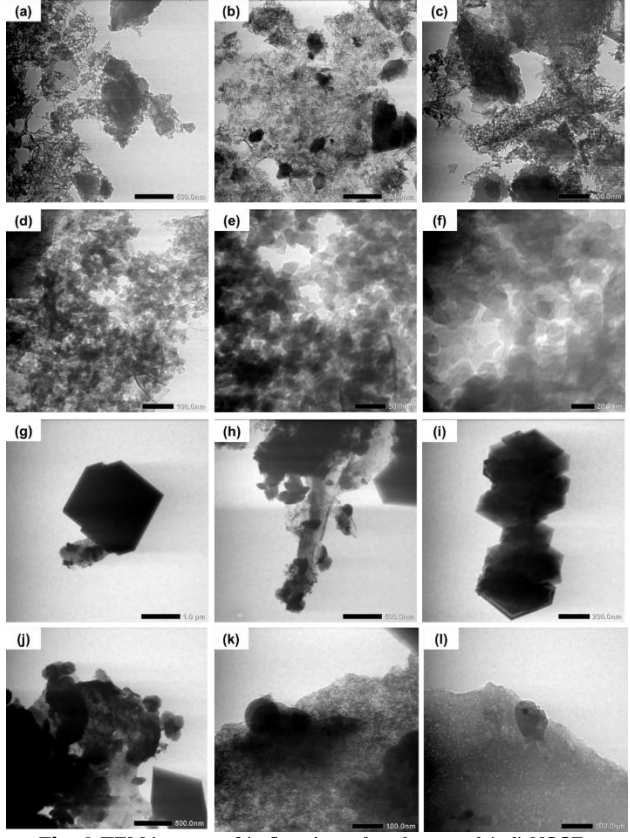
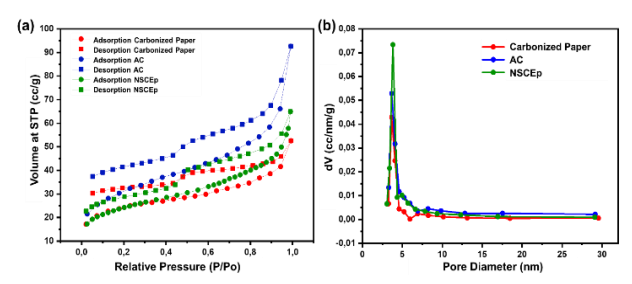


Fig. 8 TEM images of (a-f) activated carbon, and (g-l) NSCEp

Table 1
Specific Surface Area and Pore Volume of Carbonized Paper. Activated Carbon. and NSCEp

Materials	BET Surface Area (m <sup>2</sup> /g)	Total Pore Volume (cc/g)	Average Pore Diameter (nm)
Carbonized Paper	76.528	0.039	3.6592
Activated Carbon (AC)	103.932	0.093	3.6644
N/S-doped Carbon Electrode from Paper (NSCEp)	81.669	0.071	3.8192

isotherm slope signifies a stronger interaction between nitrogen and the material's surface. Among the samples, activated carbon shows the steepest slope compared to carbon and NSCEp. The specific surface area and pore volume of carbonized material activated carbon, and NSCEp is shown in Table 1. The Brunauer-Emmett-Teller (BET) analysis reveals that the specific surface areas of carbonized paper, activated carbon, and NSCEp are 76.528 m<sup>2</sup>/g, 103.932 m<sup>2</sup>/g, and 81.669 m<sup>2</sup>/g, respectively. The pore diameters for carbonized paper, activated carbon, and NSCE are 3.6592 nm, 3.6644 nm, and 3.8192 nm, respectively. It is also supported by the pore size distribution curves (based on Barrett-Joyner-Halenda (BJH) data) of carbonized paper, AC, and NSCEp as shown in Fig. 9 (b). The carbonized paper, AC, and NSCEp have a pore size diameter of approximately 3-30 nm, which is classified as mesopore (ranging from 2 to 50 nm) (Rahmawati et al., 2023). The increase in the specific surface area of activated carbon confirms the activation process, which leads to a larger surface area and pore volume. This is due to the removal of impurities and the addition of active sites.



**Fig 9.** (a) Adsorption-desorption isotherm and (b) pore size distribution curves of carbonized paper, activated carbon (AC), and NSCE<sub>D</sub>

To understand the effect of N/S doping on the prepared carbon, an impedance measurement was conducted at 20~Hz-110~kHz. The results are presented in Fig. 10 and Table 2. It was observed that activated carbon doped with nitrogen and Sulphur (NSCEp) exhibited lower resistance than undoped activated carbon. The conductivity of activated carbon (AC) was

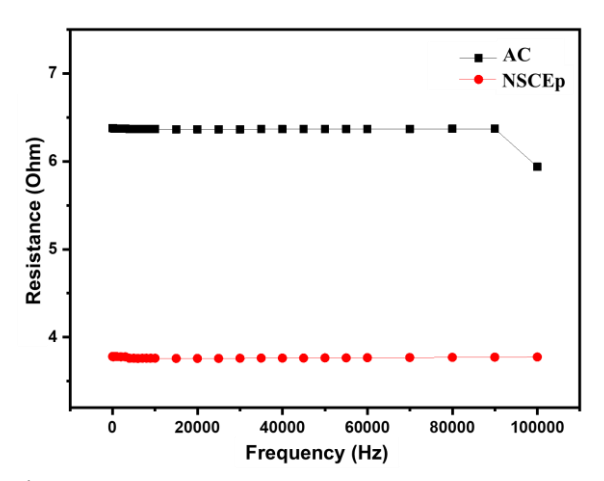


Fig. 10 The frequency and resistance curve of activated carbon (AC) and NSCEp

**Table 2**The Resistance and Conductivity Data in Various Frequency of AC and NSCEp

Material	Frequency	Resistance $(\Omega)$	Conductivity (S/cm)
AC	20 Hz	6.379	71.880
	2000 Hz	6.373	71.959
	100 kHz	5.937	77.241
NSCEp	20 Hz	3.778	121.366
	2000 Hz	3.775	121.455
	100 kHz	3.773	121.520

found to be 71.880 S/cm and 77.241 S/cm at frequencies of 20 Hz and 100 kHz, respectively, with corresponding resistances of 6.379  $\Omega$  and 5.937  $\Omega$ . Meanwhile, the NSCEp sample showed conductivity values of 121.366 S/cm and 121.520 S/cm, with resistances of 3.778  $\Omega$  and 3.773  $\Omega$  at the same frequencies. Even though at a high frequency of 100 kHz, AC shows a drop resistance of around 300  $\Omega$ , due to the high pulse frequency able to oscillate the available ions within the AC network to migrate, providing ionic conductivity. However, the resistance is still much higher than NSCEp resistance at 100 kHz. These findings align with previous studies, showing that N/S-doped carbon has higher conductivity than undoped carbon (Amalia, 2023). Consequently, the NSCEp material demonstrates more excellent suitability as an electrode for the electric double-layer capacitor in this study.

#### 3.2. Electrochemical Performance of NSCEp for EDLC Applications

The electrochemical characteristics of NSCEp were analyzed using fully fabricated EDLC cells. Cyclic voltammetry (CV) was employed to investigate the charge storage and transfer behaviors while measuring capacitance at different scan rates of 20, 30, 40, and 50 mV/s. The CV curves presented in Fig. 11 display an asymmetric shape, with a quasi-rectangular form in the lower section and a leaf-like shape in the upper region. The quasi-rectangular shape indicates the EDLC behaviour of the porous carbon materials, while the leaf-like shape may be attributed to the resistive effect caused by uneven pore distribution (Asnawi *et al.*, 2020; Yuan *et al.*, 2020).

The absence of peaks further explained that the system did not undergo any redox (reduction-oxidation) reaction. This lack of redox plateaus confirms the absence of pseudocapacitive occurrence and highlights the system's excellent performance (Rustamaji, Prakoso, Devianto, Widiatmoko, & Kurnia, 2023; Wan *et al.*, 2019). The energy storage mechanism in electric double-layer capacitors is electrostatic (non-faradaic), which means there is no charge transfer between the electrolyte and the electrode. Instead, electrolyte ions penetrate the pores of the electrode and adsorb onto its surface. When voltage is applied, the ions at the electrode-electrolyte interface become polarized, and once the voltage is removed, the electrolyte ions gradually migrate away from the interface (Jäckel *et al.*, 2016; N. Kumar, Kim, Lee, & Park, 2022).

The shape of the CV curves showed no significant deformation in the electrochemical double-layer capacitor (EDLC) across various scan rates of 20, 30, and 40 mV/s, maintaining a spindle-like shape. Even at a high scan rate of 50 mV/s, the curve remained symmetrical, although its overall form transitioned to a leaf-like shape. This change in shape is attributed to the inherent porosity of the carbon electrodes and the internal resistance encountered during the measurement (Bandaranayake, Weerasinghe, Vidanapathirana, & Perera, 2016). The stability of the spindle shape at lower scan rates indicates good performance (Li, Wang, Wei, Fan, & Yan, 2016), while the leaf-like shape at higher scan rates suggests that the increased resistance and ion movement dynamics influence the electrochemical behaviour of the EDLC.

The specific capacitance values at various scan rates for NSCE are shown in Table 3, with the highest capacitance value of 35.959 F/g achieved at a scan rate of 20 mV/s. This high capacitive performance can be attributed to the effective diffusion and charge transfer within the material's porous structure. At lower scan rates, the material exhibited near-ideal capacitive behavior. However, as the scan rate increased, the capacitance gradually decreased, suggesting that faster scan

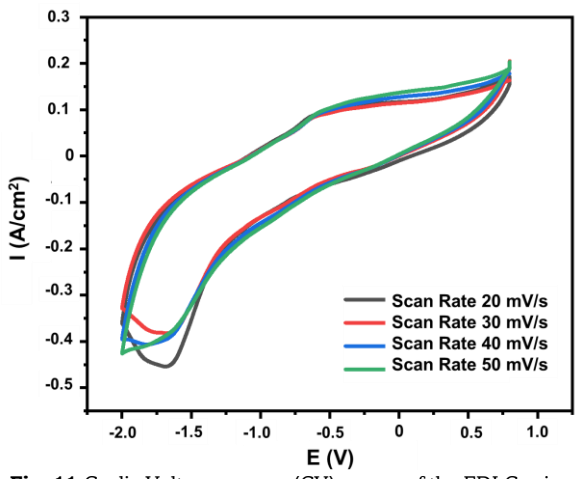


Fig. 11 Cyclic Voltammogram (CV) curves of the EDLC using NSCEp electrode at various scan rate of 20, 30, 40 and 50 mV/s within -2 V to 1 V

**Table 3**Capacitance Data of EDLC using NSCEp at various scan rate of 20, 30, 40 and 50 mV/s

Scan Rate (mV/s)	Capacitance (F/g)	
20	39.555	
30	23.234	
40	19.778	
50	14.924	

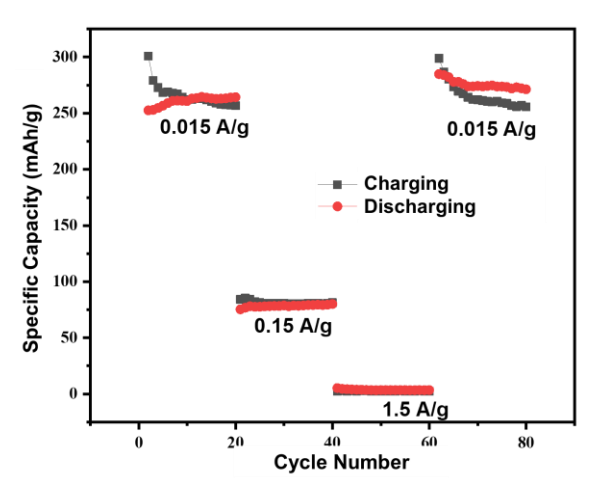
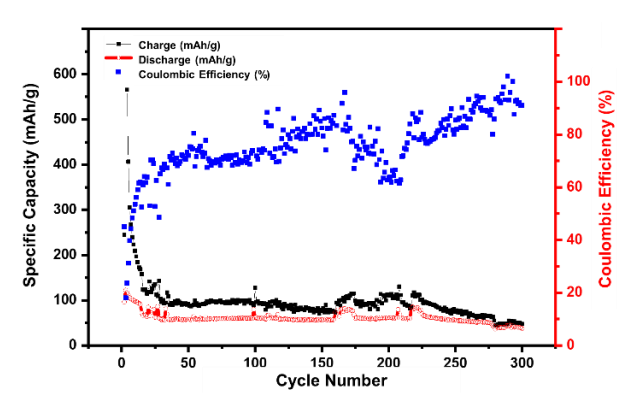


Fig. 12 Specific capacity of NSCEp EDLC at various current draws of 0.015, 0.15, and 1.5 A/g

rates hindered ion transport and adsorption within the material. This behavior is commonly observed in activated carbon materials, where higher scan rates limit the accessibility of ions to the internal pore structure due to insufficient time for ion diffusion and adsorption, thereby leading to a reduction in overall capacitance (Rustamaji *et al.*, 2023; Si *et al.*, 2013). The low specific capacitance (Cs) value at higher scan rates can be attributed to high energy loss at these rates, which results in a reduction of the number of stored charges, thereby exhibiting a lower Cs value (Muchakayala *et al.*, 2018).

Further characterization of the fabricated EDLC was performed using the Galvanostatic Charge-Discharge (GCD) profile, as shown in Figure 12, with a NEWARE battery cycler. The EDLC was tested at various current densities of 0.015, 0.15, and 1.5 A/g. The current variation was conducted sequentially, starting from 0.015 A/g, increasing to 0.15 A/g, and then to 1.5 A/g, before returning to 0.015 A/g. Each current level was tested for 20 cycles using the same EDLC cell. The results showed that the EDLC exhibited a specific capacity of 252.833 mAh/g at 0.015 A/g, 75.336 mAh/g at 0.15 A/g, and 5.183 mAh/g at 1.5 A/g. Notably, when the current returned to 0.015 A/g after 60 cycles, the specific capacity increased to 284.885 mAh/g. This indicates the electrochemical stability of the EDLC, demonstrating its ability to recover capacity even after exposure to higher current draws. The specific capacity returned to approximately 260 mAh/g when the current was adjusted back to 0.015 A/g, confirming the system's stability. This recovery is consistent with the behaviour observed in other



**Fig. 13** Cycling test performance of the NSCEp EDLC at 0.015 A/g over 300 cycles

studies on high-current-draw capacitors. Among the current densities tested, 0.015 A/g resulted in the highest specific capacity, around 280 mAh/g, which was then used for further cycle ability testing.

The cycleability test was conducted over 300 cycles, as depicted in **Fig. 13**. It shows that the EDLC exhibits an initial high specific charge capacity of 774.505 mAh/g and a discharge capacity of 139.713 mAh/g. After stabilizing at around 68 mAh/g for 200 cycles, the specific capacity gradually decreased, reaching 43.105 mAh/g after 300 cycles. The EDLC also demonstrated good coulombic efficiency, around 76.641%, throughout the charge-discharge cycles, indicating that the system maintained relatively high efficiency and performance across extended cycling. These findings suggest that the EDLC fabricated with the NSCEp electrode exhibits good performance, chemical stability, and durability over long-term cycling. Despite the decline in capacity over time, the EDLC remains efficient and reliable, particularly in low-current applications.

#### 6. Conclusion

The successful synthesis of N/S-doped Carbon Electrode from Paper Waste (NSCEp) is demonstrated through its structural, compositional, and electrochemical properties. The presence of C-N and C-S bonds confirms successful doping, while a mesoporous structure with a BET surface area of 81.67 m<sup>2</sup>/g and pore diameters ranging from 3-30 nm enhances ion transport. NSCEp exhibits high electrical conductivity, reaching 121.52 S/cm at 100 kHz, which is superior to undoped activated carbon. As an EDLC electrode, NSCEp delivers an initial specific discharge capacity of 300.56 mAh/g at 0.015 A/g, though capacity stabilizes at 68 mAh/g after 200 cycles. The coulombic efficiency of ~76.64% suggests room for improvement in energy retention. These findings indicate that NSCEp is a promising candidate for sustainable energy storage applications, with the potential for further optimization to enhance cycle stability and high-power performance.

# Acknowledgments

This research was funded by the Ministry of Higher Education, Research, and Technology through the Student Creativity Program 2023, and by Sebelas Maret University through the HRG scheme with contract number 194.2/UN27.22/PT.01.02/2024. The authors acknowledge these financial supports.

**Author Contributions**: N.A.: methodology, investigation, formal analysis; Q.R.: investigation, formal analysis; I.G.A.F.P: investigation, formal analysis; D.O.A.P.: formal analysis, writing-original draft; D.D.S.: project administration, writing-original draft; K.D.N.: data curation, writing-review & editing; E.H.: data curation, validation; Y.H.: software, validation; I.F.N: resources, writing-review & editing; I.A.T.: supervision, writing-review & editing; F.R: conceptualization, supervision, funding acquisition, writing-review & editing.

Conflicts of Interest: The authors declare no conflict of interest.

## References

Ahmad, A., & Azam, T. (2019). 4 - Water Purification Technologies. In A. M. Grumezescu & A. M. Holban (Eds.), *Bottled and Packaged Water* (pp. 83-120): Woodhead Publishing.

Ahmed, M. J., Hameed, B. H., & Khan, M. A. (2023). Recent advances on activated carbon-based materials for nitrate adsorption: A

- review. Journal of Analytical and Applied Pyrolysis, 169, 105856. https://doi.org/10.1016/j.jaap.2022.105856
- Ait El Fakir, A., Anfar, Z., Enneiymy, M., Jada, A., & El Alem, N. (2022). New insights into N, S doped carbon from conjugated polymers for efficient persulfate activation: Role of hydrogel beads in enhancement of stability. *Chemical Engineering Journal*, 442, 136055. https://doi.org/10.1016/j.cej.2022.136055
- Alahabadi, A., Singh, P., Raizada, P., Anastopoulos, I., Sivamani, S., Dotto, G. L., Landarani, M., Ivanets, A., Kyzas, G. Z., & Hosseini-Bandegharaei, A. (2020). Activated carbon from wood wastes for the removal of uranium and thorium ions through modification with mineral acid. *Colloids and Surfaces A: Physicochemical and Engineering Aspects*, 607, 125516. https://doi.org/10.1016/j.colsurfa.2020.125516
- Amalia, A. F. (2023). Doping Ganda N/S Pada Karbon Dari Bagasse Sebagai Elektroda Baterai Ion Sodium. (Bachelor Thesis). Retrieved from digilib.uns.ac.id
- Aouay, F., Attia, A., Dammak, L., Ben Amar, R., & Deratani, A. (2024). Activated Carbon Prepared from Waste Coffee Grounds: Characterization and Adsorption Properties of Dyes. *Materials*, 17(13). https://doi.org/10.3390/ma17133078
- Arumugam, B., Mayakrishnan, G., Subburayan Manickavasagam, S. K., Kim, S. C., & Vanaraj, R. (2023). An Overview of Active Electrode Materials for the Efficient High-Performance Supercapacitor Application. *Crystals*, 13(7). https://doi.org/10.3390/cryst13071118
- Asnawi, A. S. F. M., Aziz, S. B., Saeed, S. R., Yusof, Y. M., Abdulwahid, R. T., Al-Zangana, S., Karim, W. O., & Kadir, M. F. Z. (2020). Solid-State EDLC Device Based on Magnesium Ion-Conducting Biopolymer Composite Membrane Electrolytes: Impedance, Circuit Modeling, Dielectric Properties and Electrochemical Characteristics. *Membranes*, 10(12). https://doi.org/10.3390/membranes10120389
- Bandaranayake, C. M., Weerasinghe, W. A. D. S. S., Vidanapathirana, K. P., & Perera, K. S. (2016). A Cyclic Voltammetry study of a gel polymer electrolyte based redox-capacitor. Sri Lankan Journal of Physics. https://doi.org/10.4038/sljp.v16i1.8026
- Boulanger, N., Talyzin, A. V., Xiong, S., Hultberg, M., & Grimm, A. (2024). High surface area activated carbon prepared from woodbased spent mushroom substrate for supercapacitors and water treatment. *Colloids and Surfaces A: Physicochemical and Engineering Aspects,* 680, 132684. https://doi.org/10.1016/j.colsurfa.2023.132684
- Chai, L., Wang, P., Liu, X., Sun, Y., Li, X., & Pan, J. (2022). Accurately control the micropore/mesopore ratio to construct a new hierarchical porous carbon with ultrahigh capacitance and rate performance. *Journal of Power Sources*, 532, 231324. https://doi.org/10.1016/j.jpowsour.2022.231324
- Chen, J., Lin, J., Luo, J., Tian, Z., Zhang, J., Sun, S., Shen, Y., & Ma, R. (2025). Enhanced CO2 capture performance of N, S co-doped biochar prepared by microwave pyrolysis: Synergistic modulation of microporous structure and functional groups. *Fuel, 379*, 132987. https://doi.org/10.1016/j.fuel.2024.132987
- Chen, L., Chen, Y., Zeng, L., Xu, C., Li, X., Liu, Y., Ouyang, J., Sun, J., Zhou, B., & Hou, Z. (2024). Synthesis of 3D FeS embedded into N, S co-doped carbon nanotube/graphene framework for electrochemical application. *International Journal of Hydrogen Energy,* 78, 1016-1023. https://doi.org/10.1016/j.ijhydene.2024.06.390
- Chen, M., Le, T., Zhou, Y., Kang, F., & Yang, Y. (2020). Thiourea-Induced N/S Dual-Doped Hierarchical Porous Carbon Nanofibers for High-Performance Lithium-Ion Capacitors. *ACS Applied Energy Materials*, 3(2), 1653-1664. https://doi.org/10.1021/acsaem.9b02157
- Chen, Y., Guo, X., Liu, A., Zhu, H., & Ma, T. (2021). Recent progress in biomass-derived carbon materials used for secondary batteries. Sustainable Energy & Fuels, 5(12), 3017-3038. https://doi.org/10.1039/D1SE00265A
- Chen, Y., Hu, R., Qi, J., Sui, Y., He, Y., Meng, Q., Wei, F., & Ren, Y. (2019). Sustainable synthesis of N/S-doped porous carbon sheets derived from waste newspaper for high-performance asymmetric supercapacitor. *Materials Research Express*, 6(9), 095605. https://doi.org/10.1088/2053-1591/ab2d97

- Cheng, J., Bi, C., Zhou, X., Wu, D., Wang, D., Liu, C., & Cao, Z. (2023). Preparation of Bamboo-Based Activated Carbon via Steam Activation for Efficient Methylene Blue Dye Adsorption: Modeling and Mechanism Studies. *Langmuir*, *39*(39), 14119-14129. https://doi.org/10.1021/acs.langmuir.3c01972
- Chiang, C.-H., Chen, J., & Lin, J.-H. (2020). Preparation of pore-size tunable activated carbon derived from waste coffee grounds for high adsorption capacities of organic dyes. *Journal of Environmental Chemical Engineering*, 8(4), 103929. https://doi.org/10.1016/j.jece.2020.103929
- Chipembere, F., Biswick, T., & Vunain, E. (2024). Adsorptive removal of cypermethrin from aqueous solution on activated carbon derived from tobacco stem wastes: equilibrium and kinetic studies. *Journal of the Iranian Chemical Society*, 21(1), 179-191. https://doi.org/10.1007/s13738-023-02916-5
- Çiftçi, H., Çalışkan, Ç. E., İçtüzer, Y., & Arslanoğlu, H. (2024). Application of activated carbon obtained from waste vine shoots for removal of toxic level Cu(II) and Pb(II) in simulated stomach medium. *Biomass Conversion and Biorefinery*, 14(16), 18593-18605. https://doi.org/10.1007/s13399-023-03774-0
- Cui, H., Xu, J., Shi, J., Yan, N., Zhang, C., & You, S. (2022). N, S co-doped carbon spheres synthesized from glucose and thiourea as efficient CO2 adsorbents. *Journal of the Taiwan Institute of Chemical Engineers*, 138, 104441. https://doi.org/10.1016/j.jtice.2022.104441
- Dhakal, G., Mohapatra, D., Kim, Y.-I., Lee, J., Kim, W. K., & Shim, J.-J. (2022). High-performance supercapacitors fabricated with activated carbon derived from lotus calyx biowaste. *Renewable Energy*, 189, 587-600. https://doi.org/10.1016/j.renene.2022.01.105
- Domínguez-Ramos, L., Prieto-Estalrich, A., Malucelli, G., Gómez-Díaz, D., Freire, M. S., Lazzari, M., & González-Álvarez, J. (2022). N- and S-Doped Carbons Derived from Polyacrylonitrile for Gases Separation.

  Sustainability, 14(7). https://doi.org/10.3390/su14073760
- Duan, C., Meng, M., Huang, H., Wang, H., Zhang, Q., Gan, W., Ding, H., Zhang, J., Tang, X., & Pan, C. (2023). Performance and characterization of bamboo-based activated carbon prepared by boric acid activation. *Materials chemistry and physics*, 295, 127130. https://doi.org/10.1016/j.matchemphys.2022.127130
- Gakis, G. P., Termine, S., Trompeta, A.-F. A., Aviziotis, I. G., & Charitidis, C. A. (2022). Unraveling the mechanisms of carbon nanotube growth by chemical vapor deposition. *Chemical Engineering Journal*, 445, 136807. https://doi.org/10.1016/j.cej.2022.136807
- Gao, F., Zhang, D., Zhang, H., Gao, C., Huang, G., Zhang, Z., Liu, Y., Wang, Y., Terrones, M., & Wang, Y. (2024). Liquid bath-assisted combustion activation preparation of nitrogen/sulfur-doped porous carbon for sodium-ion battery applications. *Carbon, 229*, 119481. https://doi.org/10.1016/j.carbon.2024.119481
- Gao, Y., Yue, Q., Gao, B., & Li, A. (2020). Insight into activated carbon from different kinds of chemical activating agents: A review. *Science of The Total Environment*, 746, 141094. https://doi.org/10.1016/j.scitotenv.2020.141094
- Gergeroglu, H., & Ebeoglugil, M. F. (2022). Investigation of the effect of catalyst type, concentration, and growth time on carbon nanotube morphology and structure. *Carbon Letters*, *32*(7), 1729-1743. https://doi.org/10.1007/s42823-022-00381-3
- Ghafourian, H., Zare, K., Sharif, A., & Zamani, Y. (2019). Surface characteristics of different wood and coal-based activated carbons for preparation of carbon molecular sieve. *Journal of the Mexican Chemical Society*, 63(2), 120-129.
- Gonçalves Jr, A. C., Zimmermann, J., Schwantes, D., Dias de Oliveira, V. H., Dudczak, F. d. C., Tarley, C. R. T., Prete, M. C., & Snak, A. (2023). Recycling of tobacco wastes in the development of ultrahigh surface area activated carbon. *Journal of Analytical and Applied Pyrolysis*, 171, 105965. https://doi.org/10.1016/j.jaap.2023.105965
- Gopalakrishnan, A., & Badhulika, S. (2020). Effect of self-doped heteroatoms on the performance of biomass-derived carbon for supercapacitor applications. *Journal of Power Sources*, 480, 228830. https://doi.org/10.1016/j.jpowsour.2020.228830
- Gopalakrishnan, A., & Badhulika, S. (2021). From onion skin waste to multi-heteroatom self-doped highly wrinkled porous carbon nanosheets for high-performance supercapacitor device. *Journal of Energy Storage*, 38, 102533. https://doi.org/10.1016/j.est.2021.102533

- Guan, J., Fang, Y., Zhang, T., Wang, L., Zhu, H., Du, M., & Zhang, M. (2020). Kelp-Derived Activated Porous Carbon for the Detection of Heavy Metal Ions via Square Wave Anodic Stripping Voltammetry. *Electrocatalysis*, 11(1), 59-67. https://doi.org/10.1007/s12678-019-00568-9
- Hanafiah, S. F. M., Danial, W. H., Samah, M. A. A., Samad, W. Z., Susanti, D., Salim, R. M., & Majid, Z. A. (2019). Extraction and characterization of microfibrillated and nanofibrillated cellulose from office paper waste. *Malaysian Journal of Analytical Sciences*, 23(5), 901-913. https://doi.org/10.17576/mjas-2019-2305-15
- Hegde, S. S., & Bhat, B. R. (2024). Sustainable energy storage: Mangifera indica leaf waste-derived activated carbon for long-life, highperformance supercapacitors. *Rsc Advances*, 14(12), 8028-8038. https://doi.org/10.1039/D3RA08910J
- Heliani, K. R., Rahmawati, F., & Wijayanta, A. T. (2024). Screen printed carbon electrode from coconut shell char for lead ions detection. 2024, 13(1), 12. https://doi.org/10.14710/ijred.2024.57679
- Hossain, M. N., Islam, M. D., Rahaman, A., Khatun, N., & Matin, M. A. (2023). Production of cost-effective activated carbon from tea waste for tannery waste water treatment. *Applied Water Science*, *13*(3), 73. https://doi.org/10.1007/s13201-023-01879-5
- Jäckel, N., Rodner, M., Schreiber, A., Jeongwook, J., Zeiger, M., Aslan, M., Weingarth, D., & Presser, V. (2016). Anomalous or regular capacitance? The influence of pore size dispersity on double-layer formation. *Journal of Power Sources*, 326, 660-671. https://doi.org/10.1016/j.jpowsour.2016.03.015
- Jia, H., Wang, S., Sun, J., Yin, K., Xie, X., & Sun, L. (2019). Nitrogen-doped microporous carbon derived from a biomass waste-metasequoia cone for electrochemical capacitors. *Journal of alloys and compounds*, 794, 163-170. https://doi.org/10.1016/j.jallcom.2019.04.237
- Kamboj, V., & Tiwari, D. P. (2024). Removal of heavy metal (Cu, Cr, and Ni) ions from aqueous solution using derived activated carbon from water hyacinth. *Biomass Conversion and Biorefinery*, 14(4), 5075-5083. https://doi.org/10.1007/s13399-022-02702-y
- Karakilic, E., Gunaltili, E., Ekici, S., Dalkiran, A., Balli, O., & Karakoc, T. H. (2023). A Comparative Study between Paper and Paperless Aircraft Maintenance: A Case Study. Sustainability, 15(20). https://doi.org/10.3390/su152015150
- Keskin, B., Altay, B. N., Kurt, A., & Fleming, P. D. (2020). Sustainability in Paper-Based Packaging. [Kağıt Esaslı Ambalajlarda Sürdürülebilirlik]. *Gazi Mühendislik Bilimleri Dergisi, 6*(2), 129-137. Retrieved from https://dergipark.org.tr/en/pub/gmbd/issue/56490/772120
- Khan, R., Ryu, C., & In, J. B. (2024). Fabrication of modified laser-induced graphene using activated carbon and polyamic acid coating for flexible and high-performance microsupercapacitors. *Carbon*, 230, 119646. https://doi.org/10.1016/j.carbon.2024.119646
- Konukcu, A. C., & Engin, M. (2024). Shredded Waste Office Paper as a Component with Wood Particles in the Production of Particleboard. BioResources, 19(3), 5935-5948. Retrieved from https://ojs.bioresources.com/index.php/BRJ/article/view/23677
- Kumar, N., Kim, S. B., Lee, S. Y., & Park, S. J. (2022). Recent Advanced Supercapacitor: A Review of Storage Mechanisms, Electrode Materials, Modification, and Perspectives. *Nanomaterials (Basel)*, 12(20). https://doi.org/10.3390/nano12203708
- Kumar, S., Singh, P. K., Punetha, V. D., Singh, A., Strzałkowski, K., Singh, D., Yahya, M. Z. A., Savilov, S. V., Dhapola, P. S., & Singh, M. K. (2023). In-situ N/O-heteroatom enriched micro-/mesoporous activated carbon derived from natural waste honeycomb and paper wasp hive and its application in quasi-solid-state supercapacitor. *Journal of Energy Storage*, 72, 108722. https://doi.org/10.1016/j.est.2023.108722
- Kumar, V., Pathak, P., & Bhardwaj, N. K. (2020). Waste paper: An underutilized but promising source for nanocellulose mining. Waste Management, 102, 281-303. https://doi.org/10.1016/j.wasman.2019.10.041
- Łątka, J. F., Jasiołek, A., Karolak, A., Niewiadomski, P., Noszczyk, P., Klimek, A., Zielińska, S., Misiurka, S., & Jezierska, D. (2022). Properties of paper-based products as a building material in architecture An interdisciplinary review. *Journal of Building Engineering*, 50, 104135. https://doi.org/10.1016/j.jobe.2022.104135

- Li, Y., Wang, G., Wei, T., Fan, Z., & Yan, P. (2016). Nitrogen and sulfur co-doped porous carbon nanosheets derived from willow catkin for supercapacitors. *Nano Energy*, 19, 165-175. https://doi.org/10.1016/j.nanoen.2015.10.038
- Lim, J. M., Jang, Y. S., Van, T. N. H., Kim, J. S., Yoon, Y., Park, B. J., Seo, D. H., Lee, K. K., Han, Z., Ostrikov, K. K., & Doo, S. G. (2023). Advances in high-voltage supercapacitors for energy storage systems: materials and electrolyte tailoring to implementation. *Nanoscale*Adv, 5(3), 615-626. https://doi.org/10.1039/d2na00863g
- Liu, S., Dong, K., Guo, F., Wang, J., Tang, B., Kong, L., Zhao, N., Hou, Y., Chang, J., & Li, H. (2024). Facile and green synthesis of biomass-derived N, O-doped hierarchical porous carbons for high-performance supercapacitor application. *Journal of Analytical and Applied Pyrolysis, 177*, 106278. doi:https://doi.org/10.1016/j.jaap.2023.106278
- Lobato-Peralta, D. R., Duque-Brito, E., Orugba, H. O., Arias, D. M., Cuentas-Gallegos, A. K., Okolie, J. A., & Okoye, P. U. (2023). Sponge-like nanoporous activated carbon from corn husk as a sustainable and highly stable supercapacitor electrode for energy storage. *Diamond and Related Materials*, 138, 110176. doi:https://doi.org/10.1016/j.diamond.2023.110176
- Luo, X., Zhang, W., Han, Y., Chen, X., Zhu, L., Tang, W., Wang, J., Yue, T., & Li, Z. (2018). N,S co-doped carbon dots based fluorescent "onoff-on" sensor for determination of ascorbic acid in common fruits. Food Chemistry, 258, 214-221. doi:https://doi.org/10.1016/j.foodchem.2018.03.032
- Ma, X., Yuan, S., Yang, L., Li, L., Zhang, X., Su, C., & Wang, K. (2013). Fabrication and potential applications of CaCO3–lentinan hybrid materials with hierarchical composite pore structure obtained by self-assembly of nanoparticles. *CrystEngComm*, 15(41), 8288-8299. https://doi.org/10.1039/C3CE41275J
- Man, Y., Yan, Y., Wang, X., Ren, J., Xiong, Q., & He, Z. (2023).

  Overestimated carbon emission of the pulp and paper industry in China. *Energy*, 273, 127279. https://doi.org/10.1016/j.energy.2023.127279
- Manandhar, S., Shrestha, B., Sciortino, F., Ariga, K., & Shrestha, L. K. (2022). Recycling Waste Paper for Further Implementation: XRD, FTIR, SEM, and EDS Studies. *Journal of Oleo Science*, 71(4), 619-626. https://doi.org/10.5650/jos.ess21396
- Manimekala, T., Sivasubramanian, R., Karthikeyan, S., & Dharmalingam, G. (2023). Biomass derived activated carbon-based high-performance electrodes for supercapacitor applications. Journal of Porous Materials, 30(1), 289-301. https://doi.org/10.1007/s10934-022-01338-7
- Mariah, M. A. A., Rovina, K., Vonnie, J. M., & Erna, K. H. (2023). Characterization of activated carbon from waste tea (Camellia sinensis) using chemical activation for removal of methylene blue and cadmium ions. South African Journal of Chemical Engineering, 44, 113-122. https://doi.org/10.1016/j.sajce.2023.01.007
- Md Salim, R., Asik, J., & Sarjadi, M. S. (2021). Chemical functional groups of extractives, cellulose and lignin extracted from native Leucaena leucocephala bark. Wood Science and Technology, 55(2), 295-313. https://doi.org/10.1007/s00226-020-01258-2
- Mestre, A. S., Viegas, R. M. C., Mesquita, E., Rosa, M. J., & Carvalho, A. P. (2022). Engineered pine nut shell derived activated carbons for improved removal of recalcitrant pharmaceuticals in urban wastewater treatment. *Journal of Hazardous Materials*, 437, 129319. https://doi.org/10.1016/j.jhazmat.2022.129319
- Muchakayala, R., Song, S., Wang, J., Fan, Y., Bengeppagari, M., Chen, J., & Tan, M. (2018). Development and supercapacitor application of ionic liquid-incorporated gel polymer electrolyte films. *Journal of Industrial and Engineering Chemistry*, 59, 79-89. https://doi.org/10.1016/j.jiec.2017.10.009
- Nille, O. S., Patil, A. S., Waghmare, R. D., Naik, V. M., Gunjal, D. B., Kolekar, G. B., & Gore, A. H. (2021). Chapter 11 - Valorization of tea waste for multifaceted applications: a step toward green and sustainable development. In R. Bhat (Ed.), Valorization of Agri-Food Wastes and By-Products (pp. 219-236): Academic Press.
- Olabi, A. G., Abbas, Q., Al Makky, A., & Abdelkareem, M. A. (2022). Supercapacitors as next generation energy storage devices: Properties and applications. *Energy*, 248, 123617. https://doi.org/10.1016/j.energy.2022.123617

- Oloyede, O. O., & Lignou, S. (2021). Sustainable Paper-Based Packaging: A Consumer's Perspective. *Foods*, 10(5). https://doi.org/10.3390/foods10051035
- Palanichamy, P., Venkatachalam, S., & Gupta, S. (2023). Improved recovery of cellulose nanoparticles from printed wastepaper and its reinforcement in guar gum films. *Biomass Conversion and Biorefinery*, 13(15), 14113-14125. https://doi.org/10.1007/s13399-022-02516-y
- Pameté, E., Köps, L., Kreth, F. A., Pohlmann, S., Varzi, A., Brousse, T., Balducci, A., & Presser, V. (2023). The Many Deaths of Supercapacitors: Degradation, Aging, and Performance Fading. *Advanced Energy Materials*, 13(29), 2301008. https://doi.org/10.1002/aenm.202301008
- Prasetyo, S. E., Damaraji, G. M., & Kusumawardani, S. S. (2020). A Review of The Challenges of Paperless Concept In The Society 5.0.

  International Journal of Industrial Engineering and Engineering Management, 2(1), 15 24. https://doi.org/10.24002/ijieem.v2i1.3755
- Qin, R., Wang, L., Cao, D., Wang, A., Wei, Y., & Li, J. (2022). Thermal simulation experimental study on the difference of molecular structure evolution between vitrinite and inertinite in low-rank coal. Frontiers in Earth Science, 10. https://doi.org/10.3389/feart.2022.992017
- Rahmawati, F., Amalia, A. F., Ridassepri, A. F., Nakamura, J., & Lee, Y. (2024). A Functional N/S-doped Carbon Electrode from a Carbonized Bagasse Activated with Water Vapor. *J. Electrochem. Sci. Technol, 15*(4), 466-475. https://doi.org/10.33961/jecst.2024.00017
- Rahmawati, F., Heliani, K. R., Wijayanta, A. T., Zainul, R., Wijaya, K., Miyazaki, T., & Miyawaki, J. (2023). Alkaline leaching-carbon from sugarcane solid waste for screen-printed carbon electrode. *Chemical Papers*, 77(6), 3399-3411. https://doi.org/10.1007/s11696-023-02712-8
- Rahmawati, F., Ridassepri, A. F., Chairunnisa, Wijayanta, A. T., Nakabayashi, K., Miyawaki, J., & Miyazaki, T. (2021). Carbon from Bagasse Activated with Water Vapor and Its Adsorption Performance for Methylene Blue. *Applied Sciences*, 11(2). https://doi.org/10.3390/app11020678
- Rajpurohit, A. S., Punde, N. S., Rawool, C. R., & Srivastava, A. K. (2019). Fabrication of high energy density symmetric supercapacitor based on cobalt-nickel bimetallic tungstate nanoparticles decorated phosphorus-sulphur co-doped graphene nanosheets with extended voltage. *Chemical Engineering Journal*, 371, 679-692. https://doi.org/10.1016/j.cej.2019.04.100
- Revathi, A., Palanisamy, P. N., Boopathiraja, R., & Sudha, D. (2024). Heterostructure of Fe2O3 doped Alstonia Scholaris wood waste derived activated carbon based electrode for supercapacitor applications. *Diamond and Related Materials*, 144, 110953. https://doi.org/10.1016/j.diamond.2024.110953
- Ridassepri, A., Rahmawati, F., Raras Heliani, K., Somad, C., Miyawaki, J., & Wijayanta, A. (2020). Activated Carbon from Bagasse and its Application for Water Vapor Adsorption. *Evergreen*, 7, 409-416. https://doi.org/10.5109/4068621
- Rudra, S., Seo, H. W., Sarker, S., & Kim, D. M. (2024). Supercapatteries as Hybrid Electrochemical Energy Storage Devices: Current Status and Future Prospects. *Molecules*, 29(1). https://doi.org/10.3390/molecules29010243
- Rustamaji, H., Prakoso, T., Devianto, H., Widiatmoko, P., Febriyanto, P., & Eviani, M. (2024). Modification of hydrochar derived from palm waste with thiourea to produce N, S co-doped activated carbon for supercapacitor. Sustainable Chemistry for the Environment, 7, 100132. https://doi.org/10.1016/j.sceny.2024.100132
- Rustamaji, H., Prakoso, T., Devianto, H., Widiatmoko, P., & Kurnia, K. A. (2023). Facile synthesis of N, S-modified activated carbon from biomass residue for promising supercapacitor electrode applications. *Bioresource Technology Reports*, 21, 101301. https://doi.org/10.1016/j.biteb.2022.101301
- Samage, A., Halakarni, M., Yoon, H., & Sanna Kotrappanavar, N. (2024). Sustainable conversion of agricultural biomass waste into electrode materials with enhanced energy density for aqueous zinc-ion hybrid capacitors. *Carbon*, *219*, 118774. https://doi.org/10.1016/j.carbon.2023.118774

- Saputra, A. Z. D., Rhohman, F., & Fauzi, A. S. (2022). Analisa Pengolahan Sampah Kertas Menjadi Bahan Baku Dalam Industri Kertas di Indonesia. Universitas Nusantara PGRI Kediri,
- Saputri, D. D., Jan'ah, A. M., & Saraswati, T. E. (2020). Synthesis of Carbon Nanotubes (CNT) by Chemical Vapor Deposition (CVD) using a biogas-based carbon precursor: A review. *IOP Conference Series: Materials Science and Engineering*, 959(1), 012019. https://doi.org/10.1088/1757-899X/959/1/012019
- Scialla, S., Carella, F., Dapporto, M., Sprio, S., Piancastelli, A., Palazzo, B., Adamiano, A., Degli Esposti, L., Iafisco, M., & Piccirillo, C. (2020). Mussel Shell-Derived Macroporous 3D Scaffold: Characterization and Optimization Study of a Bioceramic from the Circular Economy. *Marine Drugs*, 18(6). https://doi.org/10.3390/md18060309
- Şen, U., Rodrigues, J. F. G., Almeida, D., Fernandes, Â., Gonçalves, M., Martins, M., Santos, D. M. F., & Pereira, H. (2024). Pine Nutshells and Their Biochars as Sources of Chemicals, Fuels, Activated Carbons, and Electrode Materials. *Processes*, 12(8). https://doi.org/10.3390/pr12081603
- Sharma, S., & Chand, P. (2023). Supercapacitor and electrochemical techniques: A brief review. *Results in Chemistry*, 5, 100885. https://doi.org/10.1016/j.rechem.2023.100885
- Si, W., Zhou, J., Zhang, S., Li, S., Xing, W., & Zhuo, S. (2013). Tunable N-doped or dual N, S-doped activated hydrothermal carbons derived from human hair and glucose for supercapacitor applications. *Electrochimica Acta*, 107, 397-405. https://doi.org/10.1016/j.electacta.2013.06.065
- Singh, A. K., Kumar, A., & Chandra, R. (2022). Environmental pollutants of paper industry wastewater and their toxic effects on human health and ecosystem. *Bioresource Technology Reports, 20*, 101250. https://doi.org/10.1016/j.biteb.2022.101250
- Singla, M. K., Gupta, J., Safaraliev, M., Nijhawan, P., Oberoi, A. S., & Menaem, A. A. (2024). Characterization of an activated carbon electrode made from coconut shell precursor for hydrogen storage applications. *International Journal of Hydrogen Energy*, 61, 1417-1428. https://doi.org/10.1016/j.ijhydene.2024.02.341
- Soleymani, J., Shafiei-Irannejad, V., Hamblin, M. R., Hasanzadeh, M., Somi, M. H., & Jouyban, A. (2021). Applications of advanced materials in bio-sensing in live cells: Methods and applications. *Materials Science and Engineering: C, 121*, 111691. https://doi.org/10.1016/j.msec.2020.111691
- Suhas, Gupta, V. K., Carrott, P. J. M., Singh, R., Chaudhary, M., & Kushwaha, S. (2016). Cellulose: A review as natural, modified and activated carbon adsorbent. *Bioresource Technology*, 216, 1066-1076. https://doi.org/10.1016/j.biortech.2016.05.106
- Tonoya, T., Ando, H., Takeichi, N., Senoh, H., Kojima, T., Hinago, H., Matsui, Y., & Ishikawa, M. (2023). Capacity Decay Mechanism of Lithium–Sulfur Batteries Using a Microporous Activated Carbon–Sulfur Composite as the Cathode Material. *The Journal of Physical Chemistry C, 127*(21), 10038-10044. https://doi.org/10.1021/acs.jpcc.3c01961
- Tumimomor, F., Maddu, A., & Pari, G. (2017). Pemanfaatan Karbon Aktif Dari Bambu Sebagai Elektroda Superkapasitor *Jurnal Ilmiah Sains*, *17*(1), 73-79. https://doi.org/10.35799/jis.17.1.2017.15802
- Uppugalla, S., Pothu, R., Boddula, R., Desai, M. A., & Al-Qahtani, N. (2023). Nitrogen and sulfur co-doped activated carbon nanosheets for high-performance coin cell supercapacitor device with outstanding cycle stability. *Emergent Materials*, 6(4), 1167-1176. https://doi.org/10.1007/s42247-023-00503-1
- Wan, L., Wei, W., Xie, M., Zhang, Y., Li, X., Xiao, R., Chen, J., & Du, C. (2019). Nitrogen, sulfur co-doped hierarchically porous carbon from rape pollen as high-performance supercapacitor electrode. *Electrochimica Acta*, 311, 72-82. https://doi.org/10.1016/j.electacta.2019.04.106
- Wang, C., Huang, R., Sun, R., Yang, J., & Sillanpää, M. (2021). A review on persulfates activation by functional biochar for organic contaminants removal: Synthesis, characterizations, radical determination, and mechanism. *Journal of Environmental Chemical Engineering*, 9(5), 106267. https://doi.org/10.1016/j.jece.2021.106267
- Wu, Q., He, T., Zhang, Y., Zhang, J., Wang, Z., Liu, Y., Zhao, L., Wu, Y., & Ran, F. (2021). Cyclic stability of supercapacitors: materials, energy storage mechanism, test methods, and device. *Journal of*

- Materials Chemistry A, 9(43), 24094-24147. https://doi.org/10.1039/D1TA06815F
- Wu, S., Wei, D., Yin, Y., Li, Q., Wang, H., Chen, W., Jiang, Y., & Tao, X. (2021). N, S co-doped activated carbon with porous architecture derived from partial poly (2, 2'-dithiodianiline) for supercapacitors. Journal of Energy Storage, 33, 102043. https://doi.org/10.1016/j.est.2020.102043
- Yang, I., Yoo, J., Kwon, D., Choi, D., Kim, M.-S., & Jung, J. C. (2020). Improvement of a commercial activated carbon for organic electric double-layer capacitors using a consecutive doping method. *Carbon*, 160, 45-53. https://doi.org/10.1016/j.carbon.2020.01.024
- Yang, K., Fan, Q., Song, C., Zhang, Y., Sun, Y., Jiang, W., & Fu, P. (2023). Enhanced functional properties of porous carbon materials as high-performance electrode materials for supercapacitors. *Green Energy*

- and Resources, 1(3), 100030. https://doi.org/10.1016/j.gerr.2023.100030
- Yousufi, M. (2023). Exploring paperless working: A step towards low carbon footprint. *European Journal of Sustainable Development Research*, 7. https://doi.org/10.29333/ejosdr/13410
- Yuan, Q., Ma, Z., Chen, J., Huang, Z., Fang, Z., Zhang, P., Lin, Z., & Cui, J. (2020). N, S-Codoped Activated Carbon Material with Ultra-High Surface Area for High-Performance Supercapacitors. *Polymers*, 12(9). https://doi.org/10.3390/polym12091982
- Zhai, Z., Zhang, L., Du, T., Ren, B., Xu, Y., Wang, S., Miao, J., & Liu, Z. (2022). A review of carbon materials for supercapacitors. *Materials & Design, 221*, 111017.

https://doi.org/10.1016/j.matdes.2022.111017



© 2025. The Author(s). This article is an open access article distributed under the terms and conditions of the Creative Commons Attribution-ShareAlike 4.0 (CC BY-SA) International License (http://creativecommons.org/licenses/by-sa/4.0/)